HOSTED BY
ELSEVIER
CrossMark
Available online at www.sciencedirect.com
ScienceDirect
Journal of Magnesium and Alloys 2 (2014) 208–213
www.elsevier.com/journals/journal-of-magnesium-and-alloys/2213-9567

Full length article

Effect of hydrogen on the corrosion behavior of the Mg–*x*Zn alloys

Yingwei Song [a,*], En-Hou Han [a,*], Kaihui Dong [a], Dayong Shan [a], Chang Dong Yim [b], Bong Sun You [b]

[a] *Key Laboratory of Nuclear Materials and Safety Assessment, Institute of Metal Research, Chinese Academy of Sciences, Shenyang 110016, China*
[b] *Korea Institute of Materials Science, Changwon 641-831, Republic of Korea*

Received 14 July 2014; revised 8 October 2014; accepted 9 October 2014
Available online 24 November 2014

Abstract

Hydrogen evolution reaction is inevitable during the corrosion of Mg alloys. The effect of hydrogen on the corrosion behavior of the Mg–2Zn and Mg–5Zn alloys is investigated by charging hydrogen treatment. The surface morphologies of the samples after charging hydrogen were observed using a scanning electron microscopy (SEM) and the corrosion resistance was evaluated by polarization curves. It is found that there are oxide films formed on the surface of the charged hydrogen samples. The low hydrogen evolution rate is helpful to improve the corrosion resistance of Mg alloys, while the high hydrogen evolution rate can increases the defects in the films and further deteriorates their protection ability. Also, the charging hydrogen effect is greatly associated with the microstructure of Mg substrate.

Keywords: Charging hydrogen; Corrosion resistance; Mg–*x*Zn alloys; Oxide films

1. Introduction

Mg and its alloys are the lightest structure materials with high chemical activity. They are susceptible to corrosion at the actual applications [1]. Because the standard potential of pure Mg ($E^0 = -2.4\ V_{NHE}$) is much more negative than that of hydrogen reduction, it will take place hydrogen evolution reaction at the cathodic sites during the corrosion of Mg alloys [2]. In the meantime, Mg and its alloys exhibit the special features of Negative Difference Effect (NDE) and "anodic hydrogen evolution" [3,4]. The hydrogen evolution reaction will be accelerated with increasing anodic potentials. Thus, the hydrogen evolution reaction is inevitable regardless of at cathodic and anodic regions (Cathodic reaction: $2H_2O + 2e^- \rightarrow H_2 + 2OH^-$; Anodic reaction: $Mg + 2H_2O \rightarrow Mg^{2+} + H_2 + 2OH^-$ [5]). In the case of other metal materials, plenty of research results indicate that hydrogen has a very important effect on their corrosion behavior [6,7]. Hydrogen gas can permeate into the interior of metals then gather, initiating the hydrogen embrittlement phenomenon. Also, there are some studies about the effect of hydrogen on the corrosion behavior of Mg alloys. Chen et al. [8,9] found that hydrogen can result in the crack of β phases and initiation of stress corrosion crack (SCC) on AZ91 Mg alloy. Bakkar et al. [10] permeated hydrogen into Mg alloys by EIR and PIII techniques and found that the corrosion resistance of Mg alloys was improved. The research results of Zhang et al. [11] indicate that hydrogen has a dual effect on the corrosion behavior of Mg alloys. If the concentration of hydrogen is low, it can reduce the defect density of surface films and improve the corrosion resistance. On the contrary, if the content of hydrogen is high, hydrogen can deteriorate the stability of surface films and decrease the corrosion resistance. In a word, there are not consistent opinions about the

* Corresponding authors. Tel.: +86 24 23915772; fax: +86 24 23894149.
E-mail addresses: ywsong@imr.ac.cn (Y. Song), ehhan@imr.ac.cn (E.-H. Han).
Peer review under responsibility of National Engineering Research Center for Magnesium Alloys of China, Chongqing University.

http://dx.doi.org/10.1016/j.jma.2014.10.002.

function of hydrogen on the corrosion behavior of Mg alloys. Also, the effect of microstructure on the charging hydrogen effect is not clear. Thus, the surface oxide films and corrosion resistance of the Mg−2Zn and Mg−5Zn alloys after charging hydrogen treatment are investigated, aiming to disclose the role of hydrogen in the corrosion process of Mg alloys.

2. Experimental

The experimental materials used for this investigation were the extrusion Mg−2Zn and Mg−5Zn plates which were provided by Korea Institute of Materials Science (KIMS) as reported in the previous paper [12−14]. The samples were successively ground to 3000 grit paper, cleaned in alcohol, and then dried in cool air. The samples for metallographic observation were further ground to 5000 grit paper, finely polished using 1 μm diamond paste and then etched by the solution consisting of 1 g oxalic acid, 1 mL nitric acid, 1 mL acetic acid and 150 mL distilled water.

The Mg−2Zn and Mg−5Zn alloys were charged hydrogen in 0.1 M NaCl solution (pH 6.2) at the cathodic currents of −1, −5 and −10 mA for 2 h using an EG&G potentiostat model 273 (Princeton Applied Research, USA). A classical three−electrode cell was used, with a platinum plate as counter electrode, a saturated calomel electrode as reference electrode and the sample with an exposed area of 1 cm^2 as work electrode. The potentials of the charged hydrogen samples were recorded during the charging hydrogen process. 0.1 M NaCl solution was renewed after charging hydrogen, and then the polarization curve measurements were carried out immediately. The polarization measurements started from −200 mV below open circuit potential at a constant scan rate of 0.5 mV s^{-1} and were terminated until a fast increase of the anodic current density. An initial delay of 300 s was set before the polarization curve measurements. At least three electrochemical measurements were performed under the same testing conditions for ensuring the reproducibility. The polarization curves were fitted using CorrView software.

The surface morphologies of the samples after charging hydrogen treatment were observed using a Phillips XL30 scanning electron microscopy (SEM) equipped with an energy dispersive X-ray spectroscopy (EDX).

3. Results and discussion

The microstructures of the Mg−2Zn and Mg−5Zn alloys are shown in Fig. 1. Although their microstructures have been reported in our previous papers [12−14], they are shown again aiming to compare their surface morphologies with the samples after charging hydrogen treatment. In the case of the Mg−2Zn alloy, the alloying element of Zn is completely dissolved into Mg matrix and there are no precipitation phases observed. Differently, some of Zn is dissolved into Mg matrix and the rest is precipitated on the grain boundaries of the Mg−5Zn alloy. The Mg−2Zn alloy exhibits better corrosion resistance than the Mg−5Zn alloy [14].

The Mg−2Zn and Mg−5Zn alloys were charged hydrogen at the cathodic currents of −1, −5 and −10 mA for 2 h. From the optical observation of the samples during the charging hydrogen treatment, plenty of hydrogen gas bubbles escaped from the surface of Mg alloys. The hydrogen generation rate promotes with increasing cathodic charging currents. Fig. 2 shows the development of potentials with increasing cathodic charging hydrogen time of Mg−2Zn. The larger the charging hydrogen currents are, the more negative the potentials of the samples become. The development trends of the potentials can be divided into three stages. The potentials first rise in stage I and then decline in stage II, and finally tend to rise slowly in stage III except for the sample charged hydrogen at −1 mA which keeps a stable level. The slow rise of potentials in stage III means that the chemical stability of the samples is improved gradually [15]. The sample charged hydrogen at −10 mA exhibits the highest growth rate of potential in stage III, while the sample charged hydrogen at −1 mA exhibits the smallest one. Based on this case, it can conclude that the chemical stability of the Mg alloys is promoted with increasing cathodic charging hydrogen currents from −1 to −10 mA.

The surface morphologies of the Mg−2Zn alloy charged hydrogen at various cathodic currents for 2 h are shown in Fig. 3. It can find that the oxide films consisting of sheet particles are visible on the surface of the Mg−2Zn after charging hydrogen treatment. With increasing cathodic currents, the coverage percents of the oxide films increase. The oxide films are thin. But they are more obvious in the scratch

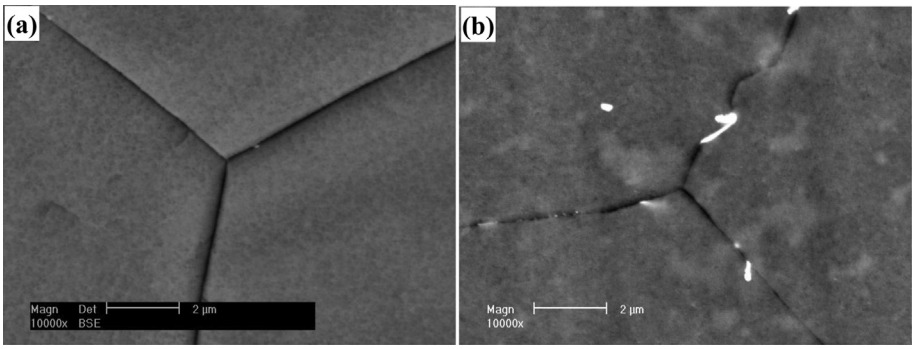

Fig. 1. Microstructure of (a) Mg−2Zn and (b) Mg−5Zn alloys.

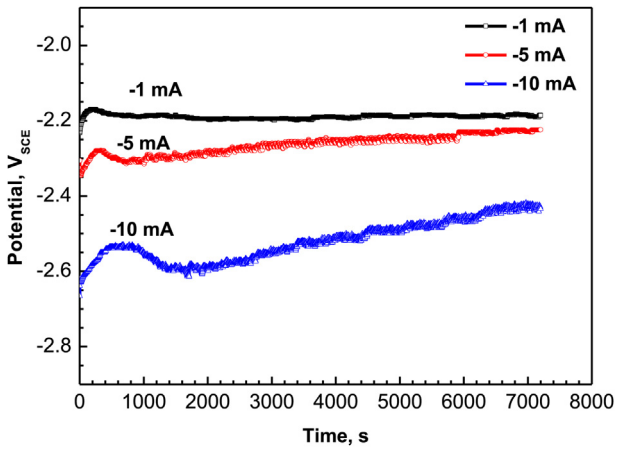

Fig. 2. $E-T$ curves of the Mg−2Zn alloy during the charging hydrogen process at various cathodic currents for 2 h (a) −1 mA; (b) −5 mA; (c) −10 mA.

regions. The chemical composition of the regions with obvious oxide films (region A in Fig. 3e) are compared with other regions (region B in Fig. 3e) by EDX as shown in Fig. 4. The regions with obvious oxide films contain a higher concentration of oxygen. Chen [9,16] reported that the chemical composition of the oxide film formed on the surface of the charged hydrogen AZ91 alloy (the charging hydrogen treatment was carried out in 0.1 M $NaSO_4$, pH 6.1) consisted of $Mg(OH)_2$ and $Al(OH)_3$ according to XPS analysis, while MgH_2 was formed in the interior of Mg substrate according to SIMS analysis. Zhang [11] mentioned the MgH_2 film on the charged hydrogen pure Mg (the charging hydrogen treatment was carried out in 0.01 M NaOH) according to M−S measurements. The charging hydrogen treatment in this paper (0.1 M NaCl, pH 6.2) is similar to the work of Chen [9,16]. Thus, the main constituent of the oxide films formed on the surface of the charged hydrogen Mg−xZn alloys should be $Mg(OH)_2$. The possible formation process of the $Mg(OH)_2$ film is suggested as follows. It is well known that hydrogen evolution reaction ($2H_2O + 2e^- \rightarrow H_2 + 2OH^-$) occurs during the cathodic charging hydrogen process. The product of OH^- can react with Mg^{2+} to form $Mg(OH)_2$ film ($Mg^{2+} + OH^- \rightarrow Mg(OH)_2$). The hydrogen generation reaction enhances with increasing cathodic currents. As a result, the local pH at the interface of Mg substrate presents stronger basicity at the higher charging hydrogen currents, resulting in

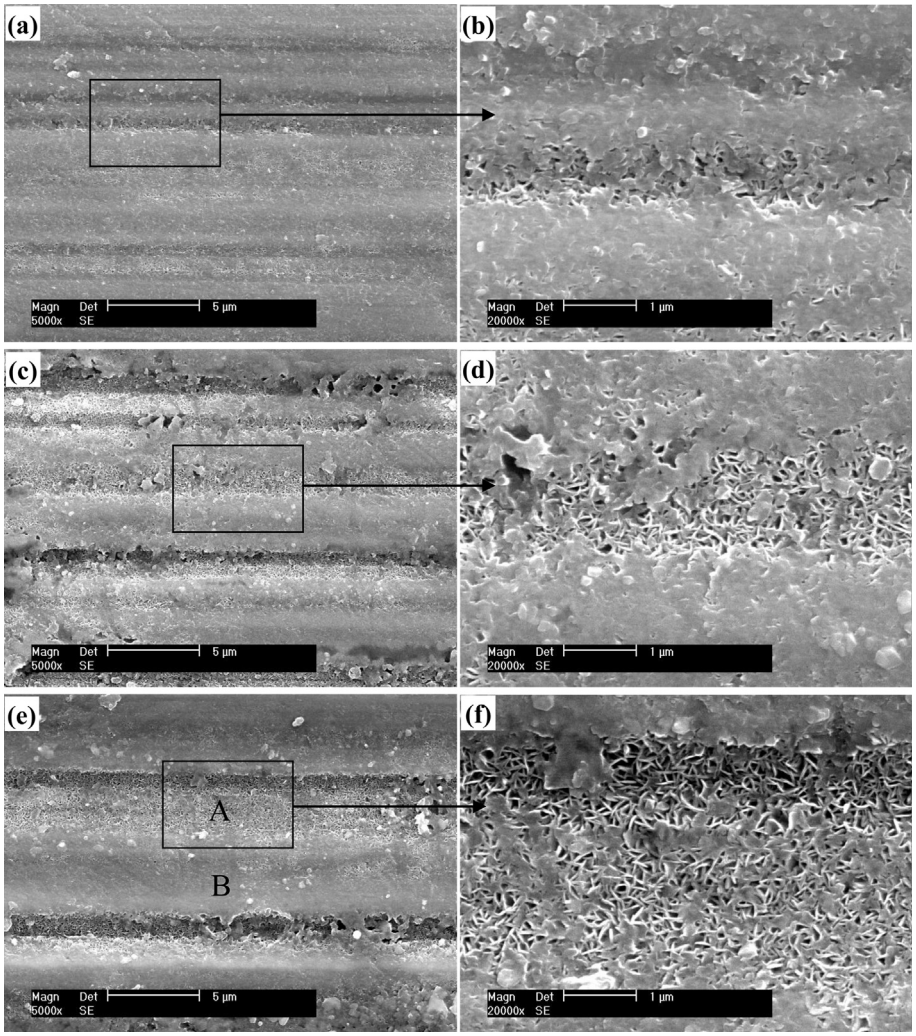

Fig. 3. Surface morphologies of the Mg−2Zn alloy charged hydrogen at various cathodic currents for 2 h (a, b) −1 mA; (c, d) −5 mA; (e, f) −10 mA.

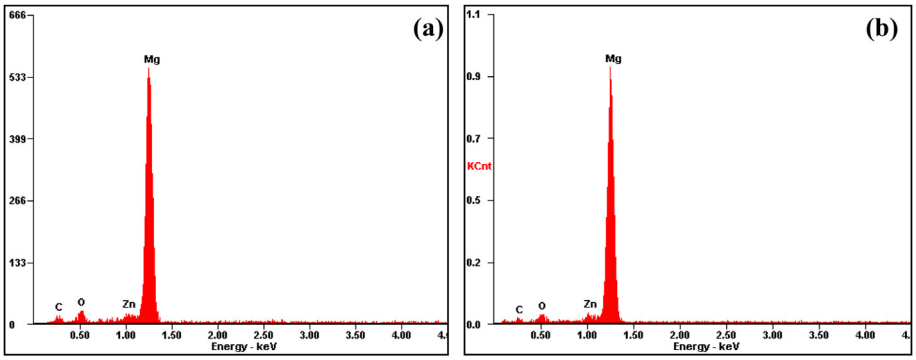

Fig. 4. EDX patterns of the product films (a) point A; (b) point B.

the easy formation of oxide films. Because the scratch regions present the higher chemical activity, the oxide films are susceptible to growth in these regions.

The corrosion resistance of the Mg−2Zn alloy after charging hydrogen at different cathodic currents is compared by polarization curves as shown in Fig. 5 and the fitting results are listed in Table 1. With the increase of charging hydrogen currents, the curves move toward the lower left corner, meaning the more negative corrosion potential (E_{corr}) and lower corrosion current density (i_{corr}). The fitting results in Table 1 also prove this case. The E_{corr} values are −1.44, 1.54 and −1.57 V (SCE) for the samples charged hydrogen at −1, −5 and −10 mA, respectively. The sample charged hydrogen at −10 mA exhibits the lowest i_{corr}, while the sample charged hydrogen at −1 mA exhibits the largest one. According to the shapes of the polarization curves, their cathodic sides have a great difference. The cathodic reaction rates decrease with the increase of charging hydrogen currents. It means that the formation of oxide films by charging hydrogen treatment is beneficial to inhibit the cathodic reaction. As for the anodic sides, slight passive trend can be observed. The samples with higher charging hydrogen currents present the longer passive regions, indicating that the oxide films can slow down the anodic dissolution reaction to some degree. The polarization

Table 1
Fitting results of the polarization curves of Mg−2Zn alloy charged hydrogen at various cathodic currents.

Samples	b_a (mV/dec)	b_c (−mV/dec)	E_{corr} (V/SCE)	i_{corr} (μA cm^{-2})
Mg−2Zn 1 mA	75.8	190.3	−1.44	32.5
Mg−2Zn 5 mA	121.6	225.2	−1.54	18.6
Mg−2Zn 10 mA	110.4	181.8	−1.57	6.5

curves demonstrate that the corrosion resistance of the samples are improved with the increase of charging hydrogen currents, which can be attributed to the inhibition effect of the oxide films on the cathodic hydrogen reaction as well as the anodic dissolution reaction.

Fig. 6 shows the development of potentials with the increase of charging hydrogen time of Mg−5Zn. It is similar to Mg−2Zn that the potentials are more negative at the higher charging hydrogen currents. But the potential of the sample charged hydrogen at −10 mA is far more negative than that of the samples charged hydrogen at −1 and −5 mA. Especially, the drastic fluctuation of the potentials can be observed at the sample charged hydrogen at −10 mA, implying that the surface status of the sample is not homogeneous.

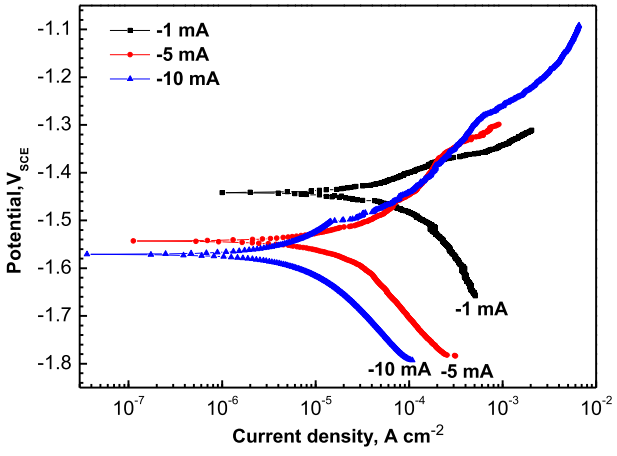

Fig. 5. Polarization curves of the charged hydrogen Mg−2Zn alloy in 0.1 M NaCl solution.

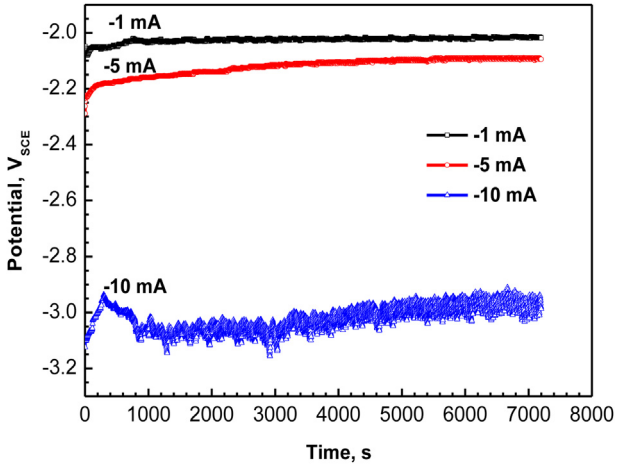

Fig. 6. E–T curves of the Mg−5Zn alloy during the charging hydrogen process at various cathodic currents for 2 h (a) −1 mA; (b) −5 mA; (c) −10 mA.

The surface morphologies of the Mg–5Zn alloy after charged hydrogen at the cathodic currents of −1, −5, and −10 mA for 2 h are shown in Fig. 7. The film on the surface of the sample charged hydrogen at −1 mA is not obvious, while the samples are completely covered by the oxide films at the charging hydrogen currents of −5 and −10 mA. The microstructures of the oxide films exhibit different characteristics from the observation of the high magnification morphologies in Fig. 7d and f. The film formed at the charging hydrogen current of −5 mA consists of flat strip particles instead of the flake particles as formed at the charging hydrogen current of −10 mA. Moreover, the film coverage percent on the Mg–5Zn alloy is higher than that on the Mg–2Zn alloy. It can be attributed to that plenty of precipitation phases on the boundaries of the Mg–5Zn alloy can increase the active regions and the films are preferentially formed on the more active surface.

The corrosion resistance of the Mg–5Zn alloy after charging hydrogen at different cathodic currents is compared by polarization curves as shown in Fig. 8 and the fitting results are listed in Table 2. The three curves show the similar cathodic sides, but there is great difference at the anodic sides. The passive trends can be observed at the samples charged hydrogen at −1 and −5 mA, especially the anodic current density is lower at the samples charged hydrogen at −5 mA. As for the sample charged hydrogen at −10 mA, it occurs Mg dissolution reaction at the anodic side and the breakdown of film can be observed at the cathodic side (Marked by arrow). The possible reasons for the similar anodic sides and different cathodic sides of the three polarization curves can be explained as follows. It is a truth that there are plenty of precipitation phases (Fig. 1b) on the gain boundaries of the Mg–5Zn alloy. The cathodic hydrogen evolution reaction is mainly associated with these precipitation phases and the effect of oxide films can be ignored. Thus, the cathodic sides of the three curves are similar. However, the oxide films formed by charging hydrogen treatment make a great contribution to the anodic reaction, namely, effectively inhibiting the anodic dissolution. As a result, the anodic sides are visible with a great difference due to the different status of the oxides films. The fitting results in Table 2 indicate that the sample charged hydrogen at −5 mA exhibits the lowest i_{corr}, while the sample

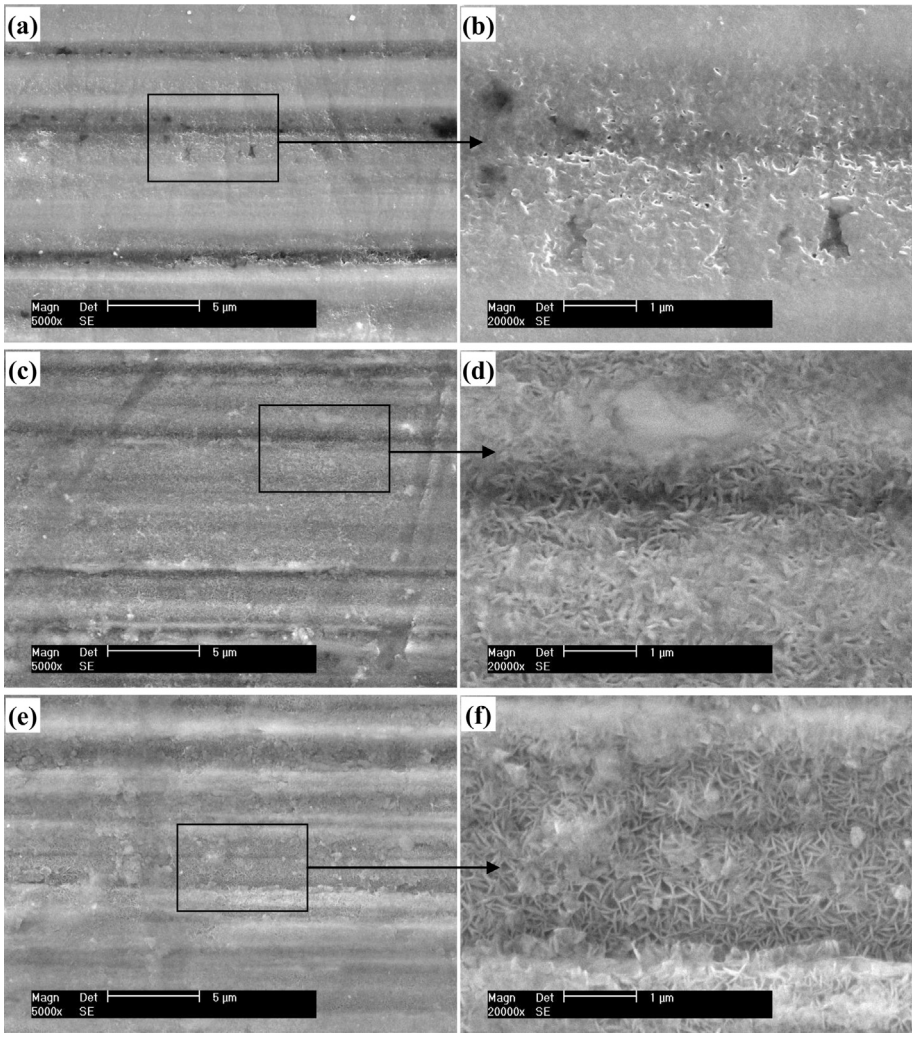

Fig. 7. Surface morphologies of the Mg–5Zn alloy charged hydrogen at various cathodic currents for 2 h (a, b) −1 mA; (c, d) −5 mA; (e, f) −10 mA.

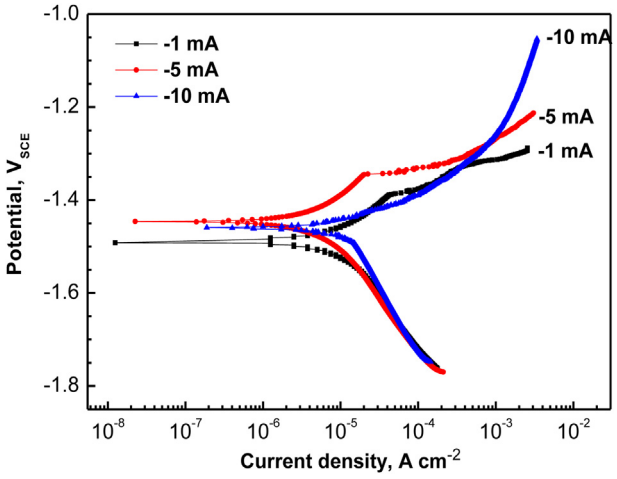

Fig. 8. Polarization curves of the charged hydrogen Mg−5Zn alloy in 0.1 M NaCl solution.

Table 2
Fitting results of the polarization curves of Mg−5Zn alloy charged hydrogen at various cathodic currents.

Samples	b_a (mV/dec)	b_c (−mV/dec)	E_{corr} (V/SCE)	i_{corr} (μA cm^{-2})
Mg−5Zn 1 mA	108.5	197.4	−1.49	5.5
Mg−5Zn 5 mA	142.5	209.2	−1.44	3.3
Mg−5Zn 10 mA	76.3	283.7	−1.46	11.8

charged hydrogen at −10 mA exhibits the largest one. The polarization curves prove that the corrosion resistance of the Mg−5Zn alloy can be improved at increasing the charging currents from −1 to 5 mA, but the corrosion resistance will reduce at the higher charging hydrogen current of −10 mA. This result is in agreement with the E−T curves in Fig. 6. The very negative potential with great fluctuation at the sample charged at −10 mA means plenty of defects in the film, which is possible due to the tearing effect by intense hydrogen evolution reaction as well as many active sites at the interface of Mg matrix and precipitation phases. Although the corrosion resistance of the Mg−2Zn alloy is improved with the increase of charging hydrogen currents of from −1 to −10 mA, maybe the corrosion resistance will reduce with further increasing cathodic charging currents to a higher level.

Thus, the above results prove that the low hydrogen evolution rate is helpful to improve the corrosion resistance of Mg alloys due to the formation of surface oxide films, while the high hydrogen evolution rate increases the defects in the films and further deteriorates their protection ability. This opinion is similar to Zhang et al. [11]. In addition, the charging hydrogen effect is greatly associated with the microstructure of Mg substrate. If the surface of Mg alloys is non-uniform with plenty of active sites, the growth rate of the oxide films formed by charging hydrogen treatment is faster but with more defects.

4. Conclusions

The effect of hydrogen on the corrosion resistance of the Mg−2Zn and Mg−5Zn alloys are investigated by charging hydrogen treatment of the both alloys at the cathodic currents of −1, −5 and −10 mA. The compact oxide films can be observed on the samples after charging hydrogen treatment, and the coverage percents of the films increase with the increase of charging hydrogen currents, especially the Mg−5Zn exhibits a faster film growth rate. The corrosion resistance of the Mg−2Zn alloy is improved with increasing cathodic charging hydrogen currents from −1 to −10 mA, while the Mg−5Zn alloy presents the best corrosion resistance at the charging hydrogen current of −5 mA. The different surface morphologies and protection ability of the oxide films can be associated with the microstructure of Mg substrate. Plenty of precipitation phases on the Mg−5Zn alloy can increase the active sites and result in more defects in the films.

Acknowledgments

Thanks for the financial support by Korea Institute of Materials Science, National Key Basic Research Program of China (No. 2013CB632205) and the National Natural Science Foundation of China (No. 51471174).

References

[1] A. Atrens, G.L. Song, F.Y. Cao, Z.M. Shi, P.K. Bowen, J. Magnesium Alloy 1 (2013) 177−200.
[2] J. Chen, J.Q. Wang, E.H. Han, W. Ke, Electrochem. Commun. 10 (2008) 577−581.
[3] G. Williams, N. Birbilis, H.N. McMurray, Electrochem. Commun. 36 (2013) 1−5.
[4] G. Song, A. Atrens, D. Stjohn, J. Nairn, Y. Li, Corros. Sci. 39 (1997) 855−875.
[5] N. Dinodi, A.N. Shetty, J. Magnesium Alloy 1 (2013) 201−209.
[6] Q. Yang, L.J. Qiao, S. Chiovelli, J.L. Luo, Corrosion 54 (1998) 628−633.
[7] M.Z. Yang, J.L. Luo, Q. Yang, L.J. Qiao, Z.Q. Qin, P.R. Norton, J. Electrochem. Soc. 146 (1999) 2107−2112.
[8] J. Chen, J.Q. Wang, E.H. Han, J.H. Dong, W. Ke, Corros. Sci. 50 (2008) 1292−1305.
[9] J. Chen, J.Q. Wang, E.H. Han, W. Ke, Mater. Sci. Eng. A 488 (2008) 428−434.
[10] A. Bakkar, V. Neubert, Corros. Sci. 47 (2005) 1211−1225.
[11] T. Zhang, Y.W. Shao, G.Z. Meng, Y. Li, F.H. Wang, Electrochim. Acta 52 (2006) 1323−1328.
[12] Y.W. Song, E.H. Han, K.H. Dong, D.Y. Shan, C.D. Yim, B.S. You, Corros. Sci. 72 (2013) 133−143.
[13] Y.W. Song, E.H. Han, D.Y. Shan, C.D. Yim, B.S. You, Corros. Sci. 60 (2012) 238−245.
[14] Y.W. Song, E.H. Han, D.Y. Shan, C.D. Yim, B.S. You, Corros. Sci. 65 (2012) 322−330.
[15] Y.W. Song, D.Y. Shan, R.S. Chen, F. Zhang, E.H. Han, Corros. Sci. 51 (2009) 62−69.
[16] Jian Chen, Jianqiu Wang, Enhou Han, Wei Ke, Mater. Sci. Eng. A 494 (2008) 257−262.